



55th Annual Midwest Student Biomedical Research Forum

Saturday, March 2, 2024

P-105

LIMITATIONS OF ELECTRONIC HEALTH RECORD SMOKING HISTORY DATA IN IDENTIFICATION OF LUNG CANCER SCREENING-ELIGIBLE PATIENTS

Presenter: Rahul Thusay, Creighton University

P-107

OPTICAL MEASUREMENTS OF GLUTAMATE RELEASE FROM ROD PHOTORECEPTOR CELLS IN MOUSE RETINA

Presenter: Lou E. Townsend, UNMC

P-109

COMPARISON OF MOLECULAR, CLINICAL, PATHOPHYSIOLOGICAL, AND PEDIGREE VARIANCE IN FAMILIES WITH HEREDITARY NONPOLYPOSIS COLORECTAL CARCINOMA (LYNCH SYNDROME) AND LYNCH-LIKE SYNDROMES

Presenter: Lavanya Uppala, Creighton University

P-110

UNIQUE GLYCOSYLATION PATTERN GOVERNS METASTATIC ORGANOTROPISM OF PANCREATIC DUCTAL ADENOCARCINOMA

Presenter: Venkatesh Varadharaj, UNMC

P-113

PIRAD TRENDS WITH URONAV PROSTATE BIOPSY: A RETROSPECTIVE STUDY

Presenter: Paul Wilkinson, Creighton University

P-114

CARM1 ARGININE METHYLTRANSFERASE AS A THERAPEUTIC TARGET FOR MEDULLOBLASTOMA

Presenter: Blayne Winkler, UNMC

P-116

CIGARETTE SMOKE EXPOSURE AND GLUCOCORTICOID INSENSIVITY OF AIRWAY SMOOTH MUSCLE CELLS

Presenter: Tianzhou Xing, Creighton University

P-117

TARGETING THE HISTAMINE RECEPTOR AXIS IN GLIOBLASTOMA

Presenter: Poonam Yadav, UNMC

TITLE: LIMITATIONS OF ELECTRONIC HEALTH RECORD SMOKING HISTORY DATA IN IDENTIFICATION OF LUNG CANCER SCREENING-ELIGIBLE PATIENTS

AUTHORS: Rahul Thusay¹; Aidan Gartner¹; Ryan Walters¹; Zachary DePew¹

¹Creighton University School of Medicine, Omaha, Nebraska

BACKGROUND: Identifying lung cancer screening-eligible patients continues to challenge clinicians even with existing USPTF guidelines. A key facet of this challenge is the collection and interpretation of patients' smoking histories, which requires accuracy of patient-reported tobacco use and comprehensive documentation in electronic health records (EHRs).

SIGNIFICANCE OF PROBLEM: Existing research shows that documented data related to tobacco use history in EHRs is frequently inconsistent or often missing critical elements that impact clinical decisions, and this has likely led to many eligible patients not receiving a screening for lung cancer. A new strategy, such as an algorithmic smoking history assessment (ASHA), is needed to increase identification of screening-eligible patients.

HYPOTHESIS: An ASHA will identify more lung cancer screening-eligible patients than the EHR data alone.

EXPERIMENTAL DESIGN: Current or former smokers between the ages of 50 to 80 attending an appointment at an outpatient pulmonology clinic were included in the study, and participants who previously received a lung cancer screening CT scan were excluded. Participating patients completed the routine visit with their provider, which included a conventional smoking history taken by the staff rooming the patient and then subsequently documented in the EHR. Following the appointment, a study team member acquired an additional tobacco smoking history from consenting patients using a simple 5-item ASHA that covered all smoking history-related items from current USPTF guidelines. Screening eligible patients were defined as current or former smokers who quit within the past 15 years with 20 pack-year smoking history or greater.

RESULTS: 91 patients were enrolled with a median age of 64 years (IQR: 57 to 72, range: 50 to 80). Analysis showed that 29 (31.9%) patients were considered screening-eligible for lung cancer based on their smoking history and quit dates via the EHR compared to 61 (67.0%) via the ASHA, which represents a pick-up rate of 35.2% (95% CI: 26.1% to 45.4%, $p < .001$). ASHA data showed statistically greater cigarettes per day, years smoked, and pack-years than EHR data (Table 1).

Table 1. Smoking History Data

Variable	EHR		ASHA		Difference		
	Median [IQR]	Range	Median [IQR]	Range	Median [IQR]	Range	p
Cigs per Day	15 [5-20]	0-60	20 [15-30]	0.3-160	6 [0-20]	-30 to 120	<.001
Years Smoked	30 [10-40]	0-60	30 [22-44]	2-60	1 [0-9]	-15 to 57	<.001
Pack Years	15 [4-40]	0-118	35 [20-54]	0.1-180	14 [1-30]	-40 to 125	<.001

CONCLUSION: This study highlights the limitations of relying solely on EHR tobacco smoking histories when identifying lung cancer screening-eligible patients. Screening for lung cancer should always result from a discussion between patients and their provider, but this is only possible if an accurate tobacco history is available to properly identify lung cancer screening eligibility. Using an ASHA to collect tobacco use histories routinely could improve identification of screening-eligible patients and initiate conversations sooner, possibly facilitating earlier detection of lung malignancies.

OPTICAL MEASUREMENTS OF GLUTAMATE RELEASE FROM ROD PHOTORECEPTOR CELLS IN MOUSE RETINA

Lou Townsend, Cody L Barta, Wallace B. Thoreson

Departments of Pharmacology & Experimental Neuroscience and Ophthalmology & Visual Sciences, University of Nebraska Medical Center, Omaha, NE 68198-5840

Background:

Vision is initiated by the capture of photons by rod photoreceptor cells in the retina. Rod light responses are transmitted to second-order bipolar and horizontal cells by changes in the ongoing rate of synaptic release of glutamate. Synaptic transmission from rods has traditionally been studied using electrophysiological techniques, but these techniques have limited ability to study release from multiple individual neurons simultaneously. The fluorescent reporter, iGluSnFr, has been used to study release from cone photoreceptors cell in mouse but fluorescence changes in rods using this reporter are too dim to be useful. We investigated the utility of using a brighter variant with improved synaptic labeling, iGluSnFr3.v857.GPI, in measuring glutamate release from rods following insertion using adeno-associated viral (AAV) or genetic constructs,

Significance of Problem:

The rate of release, diffusion, and re-uptake of glutamate in the synaptic cleft shapes transmission and our ability to see. Establishing glutamate kinetics in the context of healthy transmission is necessary before exploring any retinal diseases or disorders where transmission may be hindered.

Hypothesis:

We hypothesized that inserting the iGluSnFr3 variant into rods would provide sufficient fluorescence to detect changes in synaptic release.

Experimental Design:

AAV construct of iGluSnFr3 (AAV 2/8 Cag.iGluSnFr3.v857.GPI; Addgene #178335) was introduced via subretinal injection (n=18 retinas) and allowed to replicate for at least a week before visualizing.

Rod-specific iGluSnFr3: Using EasiCRISPR methodology, the UNMC Genome Engineering core generated mice that selectively express iGluSnFr3 in rods with expression driven by the promoter for a rod-specific gene, rhodopsin.

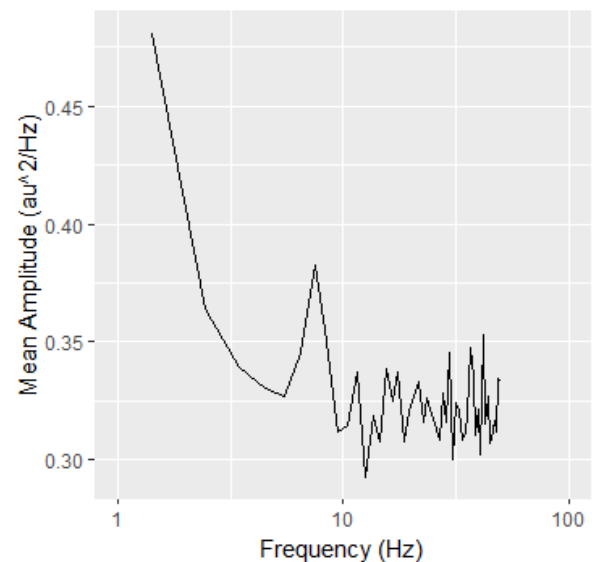
With both approaches, whole mount retinas were placed on a slide and superfused with Ames' medium. Cone terminals were labeled with PNA-conjugated rhodamine to use as a landmark. Retinas were imaged on a two-photon microscope (Scientifica) by line scans traversing individual rod terminals (2-5 ms/line). We calculated the power spectra of time-dependent fluorescence changes among individual rod terminals using ImageJ and Clampfit (Molecular Devices) software. Power spectra from different cells were averaged using a custom binning routine in R (RStudio).

Results/Data:

Rod terminals were identified by their location relative to nearby cone terminals labeled with PNA rhodamine, as well as by their characteristic shape and size. Synaptic release sites of rods sit within a membrane invagination in the rod terminal. Labeling with iGluSnFr3 therefore produced a doughnut-shaped profile when the focal plane was located at the base of the terminal. Blocking glutamate uptake with threo- β -benzyloxyaspartic acid (TBOA; 0.2 mM) caused only small changes in fluorescence intensity, with larger increases produced by addition of 2 mM glutamate. Line scans of rod terminals in darkness showed fluorescence fluctuations consistent with ongoing synaptic release. To look for different frequency components to release, we analyzed the power spectra of line scans in AAV-expressing iGluSnFr3 mice (n = 3 retinas, 57 rods). This analysis showed evidence for large changes in iGluSnFr3 fluorescence at low frequencies (<2 Hz) along with a second peak at 6-8 Hz.

Conclusions:

The peak for iGluSnFr3 fluorescence changes at 6-8 Hz is consistent with electrophysiological measurements of rod release rates at room temperature. While low frequency components below 1 Hz are largely due to dye bleaching, they might also involve slow changes in synaptic glutamate.



COMPARISON OF MOLECULAR, CLINICAL, PATHOPHYSIOLOGICAL, AND PEDIGREE VARIANCE IN FAMILIES WITH HEREDITARY NONPOLYPOSIS COLORECTAL CARCINOMA (LYNCH SYNDROME) AND LYNCH-LIKE SYNDROMES

Lavanya Uppala*, Samantha Draves*, Cynthia Watson*, Dr. Holly A. Feser Stessman*

*Creighton University, School of Medicine, Omaha, NE

BACKGROUND

Hereditary nonpolyposis colorectal carcinoma (HNPCC or Lynch syndrome) is the most common hereditary cancer syndrome, requiring diligent surveillance and tailored prevention due to its early age of onset and family-specific clinical manifestations. The etiology of HNPCC involves germline mutations of the mismatch repair system (*MLH1*, *MSH2*, *MSH6*, and *PMS2*), allowing for infidelity of DNA replication and microsatellite instability, eventually leading to cancer, predominantly of colorectal and endometrial types. With appropriate monitoring and prophylactic removal of at-risk organs, patients with Lynch syndrome may have improved prognoses. Genetic and pedigree analysis allows for one such method for identifying and verifying affected families and individuals. However, sequencing studies have shown that genetic testing alone does not always account for variability in familial presentation.

SIGNIFICANCE OF PROBLEM

Although Lynch syndrome is inherited in an autosomal dominant fashion, atypical and extracolonic manifestations may make it difficult to identify concomitant conditions. For instance, 40-60% of women may present with breast or ovarian cancer, while other cases may be attributable to other poorly understood inherited cancer syndromes. Lack of adequate explanation for rare phenotypes of HNPCC proposes the idea that other factors may be at play.

HYPOTHESIS, PROBLEM, OR QUESTION

In this review, select investigation of family pedigrees with preliminary evidence of Lynch syndrome were examined to assist in prediction and clarification of historical diagnoses, as well as provide further support for future identification of families with hereditary cancer syndromes. Moreover, investigation of individual patient charts with clinical histories significant for several neoplastic conditions allowed for the elucidation of disorders which may be somatic versus germline.

EXPERIMENTAL DESIGN

134 families with putative clinical signs of Lynch syndrome or hereditary cancer were selectively investigated based on availability of pedigree information and DNA samples from the Creighton Hereditary Cancer Center Biorepository, collected from various research studies from 1973-2014. Families with confirmed *BRCA1* or *BRCA2* clinical variants were not included in the study, and pedigree and chart analysis was confirmed using genetic sequencing. The effect of somatic versus germline mutational burden was assessed by comparing twins.

RESULTS/DATA

When combined with targeted genetic sequence analysis using customized molecular inversion probes (MIPs), we have confirmed that some variation in families thought to have Lynch syndrome may also be attributed to other hereditary cancer genes, and whether such mutations may be benign or malignant. Moreover, variant analysis of family members, including twins, has revealed significant insight into mutational burden which may explain some differences in onset and severity of inherited conditions.

CONCLUSIONS

Pedigree analysis and further confirmation with genetic studies have allowed for the elucidation of familial trends of Lynch syndrome and similar, associated inherited cancer syndromes. This provides a framework for the enhanced identification, surveillance, and genetic counseling of families. Given that this illness may present with an early age of onset, early diagnosis is crucial to improving patient outcomes.

UNIQUE GLYCOSYLATION PATTERN GOVERNS METASTATIC ORGANOTROPISM OF PANCREATIC DUCTAL ADENOCARCINOMA

Venkatesh Varadharaj¹, Frank Leon¹, Wyatt Petersen¹, Rama K Nimmakayala¹, Surinder K Batra¹, Moorthy P Ponnusamy¹
¹Department of Biochemistry and Molecular Biology, University of Nebraska Medical Center, Omaha, NE.

Background: The most common cause of mortality in cancer patients is the metastasis of neoplastic cells. Pancreatic cancer (PC) is not different in this trend, where patients majorly develop lung and liver metastasis, and an overall five-year survival rate is 12% despite advances in therapy. Glycosylation is one of the critical post-translational modifications in proteins, lipids, and even RNA that orchestrate the addition of glycan structures with the help of glycosyltransferase (GT). The expression of GTs is instrumental in modulating the phenotype of malignant cells and promoting cancer cell survival at the metastatic niche. Specifically, we found that upregulation of GCNT3 (glucosaminyl (N-acetyl) transferase 3) and B3GNT3 (beta-1,3-N-acetylglucosaminyltransferase 3) expression are key mediators in altering glycosylation patterns in PC cells and that enhance the metastatic proclivity towards liver and lung respectively. Regardless of the specific proteins exhibiting aberrant glycan signatures, probing the pattern of glycosyltransferase expression is currently a potential avenue for cancer therapy by disrupting the critical molecular factors that support tumor malignancy and metastasis.

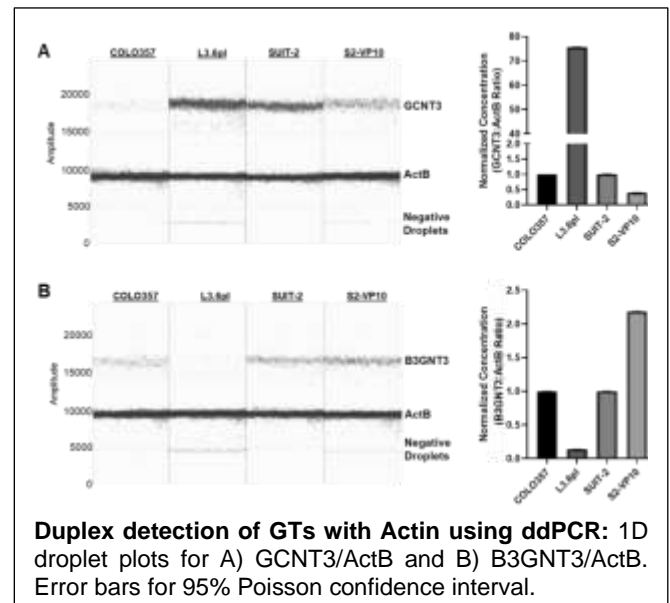
Significance of Problem: Malignant transformation of cancer cells is primarily associated with modifying tumor-cell glycosylation, a critical contributor to metastatic organotropism. However, the mechanistic underpinnings of glycosylation about organ-specific metastasis remain poorly understood. Understanding the roles of glycosyltransferases in organotropism will provide valuable targets for cancer diagnosis, prognosis, and therapy.

Hypothesis: The unique expression of GCNT3 and B3GNT3 in pancreatic cancer cells drives liver and lung-specific metastasis.

Experimental Design: The COLO357 and SUI-2 PC cells were used to develop organ-derived metastatic subline models like L3.6pl (Liver) and S2-VP10 (Lung) using orthotopic and tail vein injections of consecutive organ-enriched passages. We generated the second metastatic model by introducing a single PC cell line SUI2 into the pancreas and harvested metastatic lung and liver cells to avoid the discrepancy of different cell lines used for lung and liver metastasis in the first model. These two models replicate key aspects necessary to study the lung and liver-specific metastasis of PC. The RT² PCR array was used to analyze the gene expression of GTs in lung and liver metastatic models, providing insights into the altered GT expressions associated with metastasis. The qPCR analysis was performed on a selected panel of human GT genes involved in glycosylation modification, revealing varying GT expression levels, and focusing on two key GTs based on further validation assays. The droplet digital PCR (ddPCR) and western blot analysis were used to confirm the differential expression of GTs at both the RNA and protein levels. The GCNT3 and B3GNT3 were knocked out using the CRISPR Cas9 system to observe the difference in migratory potential. Immunohistochemistry and Immunofluorescence experiments on the primary and metastatic PC tissues validated the specific expression of GTs in lung and liver metastatic tissues.

Results: We examined the expression patterns of GCNT3 and B3GNT3 at both the RNA and protein levels to assess their roles in lung and liver-specific metastasis. An unbiased transcriptional screen revealed a reciprocal >2-fold increase in GCNT3 and B3GNT3 expression in the L3.6pl and S2-VP10 metastatic cell lines, respectively. Further, dd-PCR results showed an increased number of DNA copies for GCNT3 (>100-fold) and B3GNT3 (>3.5-fold) in L3.6pl (liver) and S2-VP10 (lung) cells, respectively, compared to the PC controls. The western blot analyses confirmed that these metastatic liver and lung clones have distinct glycosyltransferase protein expression compared to the parental pancreatic cancer cells. The CRISPR KO of GCNT3 and B3GNT3 showed significant differences in the migratory potential of the liver and lung metastatic cells. These results were further validated in human tissue from the same patient's primary pancreatic tumor and metastatic lung and liver tissues collected through the UNMC Rapid Autopsy program (UNMC-RAP). Our IHC studies on RAP tissues validated that the GCNT3 was significantly overexpressed in liver metastatic tissues, and B3GNT3 was overexpressed in lung metastatic tissues. Further, Immunofluorescence studies reflected the same expressional pattern and highlighted the clinical significance of glycosyltransferase differential expression in the metastasis of pancreatic ductal adenocarcinoma.

Conclusion: Our data suggest that a clonal population of pancreatic cancer cells that highly express GCNT3 and B3GNT3 give rise to liver and lung metastasis, respectively, and highlights the correlation between glycosylation and organ-specific metastasis.



PIRAD TRENDS WITH URONAV PROSTATE BIOPSY: A RETROSPECTIVE STUDY

Paul Wilkinson, Aidan Gaertner, Christopher Knoedler
Creighton University School of Medicine Omaha, NE

Background: Prostate cancer is the most common cancer in American men. It is usually found in men over the age of 50 and is a slow-growing, yet potentially fatal, disease. More than eighty percent of prostate cancer is detected in men over the age of 65. The ability for clinicians to accurately detect prostate cancer at an early stage in disease development can have a significant impact on patient outcome and quality of life.

UroNav is a diagnostic tool used to improve detection of clinically significant prostate cancer. The technology allows fusion of a multiparametric prostate MRI with a transrectal prostate ultrasound (MRI/TRUS) which improves accuracy of prostate biopsies. Minnesota Urology was an early adopter of this technology and the goal of this retrospective study was to evaluate the utility of UroNav-guided biopsies. The Prostate Imaging Reporting and Data System (PIRADS) score classifies MRI lesions on a scale from 1 to 5, which reflects the level of clinical suspicion of cancer from least to most. This study evaluates PIRAD trends in patients who had undergone UroNav-guided prostate biopsies.

Significance of Problem: The ability to detect prostate cancer early in patients has many effects on patient outcomes and the quality of life experienced by patients. Early detection of prostate cancer can provide more treatment options and can reduce the symptoms experienced by patients. Early detection of prostate cancer is vital in reducing the mortality rate of the disease and results in more years lived with a high quality of life for patients. Besides improving detection of cancer, the goal was to avoid performing saturation biopsies and decrease side effects of multiple biopsies. The use of MRI can help clinicians precisely locate prostate biopsy sites, leading to more accurate results. This technology can help patients avoid multiple biopsies along with the physical and emotional distress that often coincides.

Question: To evaluate the PIRAD trends in our community of over 1500 patients that underwent an UroNav prostate biopsy between January 2015 and December 2018.

Experimental Design: Prostate biopsy results from the Minnesota Urology database were retrospectively analyzed over a 3 year period. The PIRAD scores of 1500 patients were retrospectively analyzed from January 2015 to December 2018. The percent of PIRAD 3, 4, and 5 scores were broken down by year. Each PIRAD score percent cancer was also determined in this time frame by year.

Results:

PIRAD score percent breakdown by year

PIRAD	2015	2016	2017	2018
3	67	63	49	48
4	26	25	31	27
5	3	4	13	20

Percent cancer detected by PIRAD score / year

PIRAD	2015	2016	2017	2018
3	10	13	15	17
4	27	30	35	50
5	71	81	80	93

Conclusion:

Every year our ability to detect cancer advances. The use of multiparametric MRI in our community and UroNav biopsy continues to evolve and improve care for our patients. UroNav provides benefit in detecting not only prostate cancer, but clinically significant prostate cancer at a higher rate. The use of MRI has greatly advanced the ability to accurately detect prostate cancer. The data displayed that as higher PIRAD scores were detected with MRI, the likelihood of the biopsy to return with cancer increased. The use of UroNav-guided biopsies can not only help detect prostate cancer earlier, but can also help reduce potentially harmful and unnecessary biopsies for patients. These results are relevant towards clinical practice. highlighting the

CARM1 Arginine Methyltransferase As A Therapeutic Target For Medulloblastoma

Blayne C. Winkler^{1,2}, Kyle A. Rohrer^{1,2}, Nagendra K. Chaturvedi^{2,4}, Don W. Coulter^{2,4}, Hamid Band^{3,4} and Sutapa Ray^{2,4}

Molecular Genetics and Cell Biology Program¹, Department of Pediatrics², Eppley Institute³, and Child Health Research Institute⁴, University of Nebraska Medical Center, Omaha, NE

Background. Medulloblastoma (MB) is the most common primary malignant brain tumor and is the leading cause of cancer-related death among children and adolescents. Based on genomic profiling, MB is classified into four subgroups WNT, Sonic Hedgehog (SHH), Group 3 and 4. MYC-amplified Group 3 MB is the most aggressive kind and has the worst prognosis among the different subgroups of MB. Aberrantly activated signal transducers and activators of transcription-3 (STAT3) in MB acts as a key transcriptional regulator that promotes the expression of the MYC oncogene. Further, as epigenetic mechanisms play significant roles in Group 3 MB tumorigenesis, we aim to characterize and investigate the therapeutic potential of an epigenetic modifier, Coactivator Associated Arginine Methyltransferase 1 (CARM1) alone or in combination with STAT3 in high-risk MB.

Significance of Problem. Group 3 tumors are highly metastatic and have a high rate of recurrence with a very low survival rate compared to other subgroups of MB tumors. CARM1 is often overexpressed in many cancers and is an important coactivator that asymmetrically dimethylates (ASDM) arginine residues on many different cancer-associated transcription factors, histones, and non-histone substrates, thereby modulating functional activities, and promoting tumor initiation. However, there is no previous research elucidating the role of CARM1 in MB or promoting MB pathogenesis.

Hypothesis. We hypothesize that CARM1 triggers hypermethylation of its substrates including STAT3, thereby activating STAT3 and accelerating the process of MB tumorigenesis.

Experimental Design. This study aims to determine the functional role of the CARM1-STAT3 axis in MB and the efficacy of a CARM1 inhibitor alone and in combination with a STAT3 inhibitor in Group 3 MB. We will utilize co-immunoprecipitation, proximity ligation assay, cell viability assay, and Western blot to achieve our goals.

Results/Data. Screening an epigenetic drug library of 462 inhibitors that modulate the activity of a variety of epigenetic 'writers and erasers' and 'reader' proteins revealed a CARM1 inhibitor (CARM-1-IN) as the most promising modulator that consistently synergizes with the STAT3 inhibitor WP1066. Cell viability assay by luminescence revealed that treatment with CARM-1-IN alone in MB showed cytotoxic effects while the combination of CARM-1-IN and WP1066 showed a synergistic effect at multiple concentrations in MB cell lines, including Group 3. Our preliminary data by immunoprecipitation (IP)/immunoblot assay also reveals that STAT3 is asymmetrically dimethylated in MB. Furthermore, co-immunoprecipitation assay with CARM1 showed the presence of STAT3 in the immune complex indicating that endogenous CARM1 interacts with STAT3 in an MB cell line.

Conclusion. We conclude that (1) the combination treatment of CARM-1-IN and WP1066 shows a synergistic effect on MB cell viability, (2) endogenous CARM1 interacts with STAT3 and (3) STAT3 is asymmetrically dimethylated in MB. These early results suggest that STAT3 may be a direct target of CARM1 and therefore, in our future study, we would utilize a CARM1 inhibitor that would prevent CARM1-mediated methylation of STAT3 and subsequently alter transcription of STAT3 target genes including MYC in Group 3 MB. Additionally, a CARM1 inhibitor could alter ASDM arginine residues on non-histone substrates or histones that could impede the function of other important transcription factors and/or complexes that help regulate MB pathogenesis in conjunction with a STAT3 small molecular inhibitor.

CIGARETTE SMOKE EXPOSURE AND GLUCOCORTICOID INSENSITIVITY OF AIRWAY SMOOTH MUSCLE CELLS

Tianzhou Xing¹, Thomas B Casale², Yan Xie¹, Reynold A Panettieri Jr³, Peter W. Abel¹, Yaping Tu¹

¹ Department of Pharmacology and Neuroscience, Creighton University School of Medicine, Omaha, NE

² Division of Allergy and Immunology, Internal Medicine Department, Morsani College of Medicine, University of South Florida, Tampa, FL.

³ Rutgers Institute for Translational Medicine and Science, Rutgers, The State University of New Jersey, New Brunswick, NJ.

Background and Significance of Problem: Chronic obstructive pulmonary disease (COPD) is a leading cause of morbidity and mortality whereas over 300 million individuals suffer from asthma worldwide, with an additional 100 million individuals projected to be at risk. Cigarette smoking is recognized as the major risk factor in COPD and asthma patients who smoke often have poorly controlled disease. Glucocorticoids (GC) are the most effective anti-inflammatory drugs available. However, COPD and refractory severe asthma are frequently resistant to glucocorticoid therapy, thus posing an unmet need for better therapies. Although immune cells have been used to investigate glucocorticoid insensitivity (GCI), airway smooth muscle (ASM) cells have emerged as key contributors not only to airway hyperresponsiveness (AHR) but also to airway inflammation in patients with COPD and severe asthma. The objective of this study was to investigate effects of cigarette smoke exposure on glucocorticoid sensitivity of ASM cells. **Hypothesis:** Cigarette smoking exposure renders ASM cells insensitive to glucocorticoid transactivation. **Experimental Design:** Primary human ASM cells were derived from healthy controls and asthma patients. Cells were treated with various concentrations of cigarette smoking extract (CSE) for 24 h or two weeks. GC transactivation was measured using a Glucocorticoid Response Element (GRE)-driven luciferase reporter assay and measuring GC-inducible gene expression by qRT-PCR. Single-cell RNA sequencing was performed to identify differentially expressed genes (DEGs) in HASM cells and confirmed by qRT-PCR. Twenty normal nonsmoking subjects were enrolled as controls, with screening FEV₁ > 80% predicted. Forty current smokers were also enrolled, divided into subjects who demonstrated AHR, with a positive methacholine challenge (n=20) versus those without AHR (n=20). DEGs expression from peripheral blood mononuclear cells (PBMC) in chronic smokers, with and without AHR were determined by western blot assays. Data are presented as the mean ± SEM. P < 0.05 is considered to be statistically significant. **Results:** CSE treatment for 24 h impaired GRE activation and the GC induction of several anti-inflammatory genes in multiple HASM cell lines in a dose-dependent manner with 70% reduction in 5% CSE-treated HASM cells. Chronic treatment with 2.5% CSE caused transcriptomic changes in HASM cells including Regulator of G Protein Signaling 2 (RGS2), a key regulator of ASM hypercontraction and AHR in asthma. Importantly, the GC dexamethasone enhanced β 2-agonist albuterol-induced RGS2 expression in HASM cells, which was also impaired in CSE-treated HASM cells. In addition, RGS2 protein expression was significantly reduced in PBMC from chronic smokers without AHR, and to a greater degree in smokers with AHR, versus non-smokers. **Conclusions:** Our results indicate that CSE exposure not only profoundly impairs GC transactivation but also abolished dexamethasone and β 2-agonist-induced RGS2 protein expression in HASM cells. Since RGS2 upregulation is a genomic mechanism of β 2-agonist-induced bronchoprotection that is enhanced by GC, our study suggests ASM as an important target for glucocorticoid therapy and may contribute to cigarette smoking-related GC insensitivity seen in patients with COPD and severe asthma.

TITLE: TARGETING THE HISTAMINE RECEPTOR AXIS IN GLIOBLASTOMA.**Poonam Yadav**¹, Raghupathy Vengoji¹, Maneesh Jain^{1,2}, Surinder K Batra^{1,2,3}, Nicole Shonka^{3,4}.

¹Department of Biochemistry and Molecular Biology, University of Nebraska Medical Center, Omaha, NE; ²Eppley Institute for Research in Cancer and Allied Diseases, University of Nebraska Medical Center, Omaha, NE; ³Fred and Pamela Buffett Cancer Center, Omaha, NE, USA; ⁴Department of Internal Medicine, Division of Oncology & Hematology, University of Nebraska Medical Center, Omaha, NE.

Abstract:

Background: Glioblastoma (GBM) is an aggressive and lethal primary brain tumor. It accounts for 49.1% of total malignant primary brain and CNS tumors with an annual incidence rate of 3.23 per 100,000, and the 5-year survival rate is only 6.8%. It inevitably recurs even after maximal safe surgical resection, temozolomide (TMZ), and radiotherapy. Interestingly, several studies have revealed that people with a previous history of allergies, atopy, or asthma have fewer incidences of GBM. A recent study recognized that the high expression of histamine receptor 1 (HRH1) is inversely related to overall survival and progression-free survival when compared with those with low expression of HRH1 in a patient with GBM. Moreover, silencing of HRH1 reversed the immunosuppressive tumor microenvironment by switching the M2 (anti-inflammatory) to M1 (proinflammatory) phenotype in GBM.

Significance of Problem: GBM is extremely difficult to treat because of its heterogeneous nature, chemo and radiotherapy resistance development, and the blood-brain barrier's selective permeability. Despite the standard care of treatment, GBM almost always reoccurs, and we have limited treatment options to treat these patients. Therefore, there is an urgent need for additional intervention for GBM patients to increase survival outcomes.

Hypothesis: We hypothesize that brompheniramine enhances the efficacy of TMZ in GBM by inhibiting HRH1-mediated tumor growth and immunosuppression.

Experimental Design: Drug repurposing is an approach to using an already FDA-approved drug for new medical purposes. We used a bioinformatics tool, iLINCS, which analyses the transcriptomic and proteomic datasets and signatures of cellular perturbations to identify novel targets for unique therapeutic approaches. This tool identified 36 drugs that can reverse GBM signatures after analyzing 99 GBM and 38 healthy samples. Based on the concordance score and blood-brain barrier permeability, we selected brompheniramine (Brom), a first-generation HRH1 antagonist, as a potential candidate to reverse the GBM signature. HRH1 expression analysis was done on human and mouse GBM cell lines by immunoblotting. The effect of Brom alone or in combination with TMZ was investigated on proliferation, DNA damage and apoptosis of U118 and U251 human GBM cell lines and three syngeneic cell lines (EGFRvIII, p16^{-/-} & GFAP Cre (EPG), PTEN^{+/-}, p53R172H^{+/-}, EGFRvIII & GFAP Cre (PEPG), PTEN^{-/-}, p53R172H^{-/-} & GFAP Cre (PPG)). Experiments were repeated thrice and presented as mean values \pm standard deviation. Statistical analysis was performed using SAS 9.4 software (SAS Institute Inc. NC). P-values less than 0.05 were considered statistically significant.

Results/Data: Our result shows that HRH1 is expressed highly on human and syngeneic GBM cell lines and the mice GBM tissue section. The expression of HRH1 is 3 folds higher in the TMZ-resistant cell line compared to the parental cell line. Addition of histamine induces proliferation in U118 cells in a concentration-dependent manner and increases TMZ resistance. The addition of Brom decreased the proliferation of the U118 and U251 cell lines in a dose-dependent manner. The IC₂₅ concentration of Brom is 85 μ M and 15 μ M, and the IC₂₅ concentration of TMZ is 250 μ M and 30 μ M in U118 and U251 cell lines, respectively. The toxicity analysis shows that Brom was unable to decrease the proliferation of normal human astrocytes and endothelial cells, proving it is nontoxic to non-transformed cells. Combination treatment of IC₂₅ concentration of TMZ and Brom decreases proliferation in both mouse and human GBM cells. Eight-hour pretreatment with Brom increased the apoptotic efficacy of combination treatment in the U118 cell line. Our data shows that combination therapy increases DNA damage and decreases the DNA repair mechanism, possibly by downregulating the expression of O⁶methylguanine-DNA methyltransferase (MGMT).

Conclusions: Our studies suggest that Brom, in combination with TMZ, enhanced the anti-tumor efficacy of TMZ in human GBM cell lines *in vitro* by inhibiting proliferation, inducing DNA damage, and apoptosis.